buildings

MDPI

Article

Building Energy Efficiency Enhancement through Thermochromic Powder-Based Temperature-Adaptive Radiative Cooling Roofs

Ge Song, Kai Zhang *, Fei Xiao, Zihao Zhang, Siying Jiao and Yanfeng Gong

College of Urban Construction, Nanjing Tech University, Nanjing 211816, China
* Correspondence: kai.zhang.ch@njtech.edu.cn

Abstract: This paper proposes a temperature-adaptive radiative cooling (TARC) coating with simple preparation, cost effectiveness, and large-scale application based on a thermochromic powder. To determine the energy efficiency of the proposed TARC coating, the heat transfer on the surface of the TARC coating was analyzed. Then, a typical two-story residential building with a roof area of 258.43 m^2 was modeled using EnergyPlus. Finally, the energy-saving potential and carbon emission reduction resulting from the application of the proposed TARC roof in buildings under different climates in China were discussed. The results showed that the average solar reflectivity under visible light wavelengths (0.38–0.78 μm) decreases from 0.71 to 0.37 when the TARC coating changes from cooling mode to heating mode. Furthermore, energy consumption can be reduced by approximately 17.8–43.0 MJ/m^2 and 2.0–32.6 MJ/m^2 for buildings with TARC roofs compared to those with asphalt shingle roofs and passive daytime radiative cooling (PDRC) roofs, respectively. This also leads to reductions in carbon emissions of 9.4–38.0 $kgCO_2/m^2$ and 1.0–28.9 $kgCO_2/m^2$ for the buildings located in the selected cities. To enhance building energy efficiency, TARC roofs and PDRC roofs are more suitable for use on buildings located in zones with high heating demands and high cooling demands, respectively.

Keywords: temperature-adaptive roof; radiative cooling; building energy efficiency

Citation: Song, G.; Zhang, K.; Xiao, F.; Zhang, Z.; Jiao, S.; Gong, Y. Building Energy Efficiency Enhancement through Thermochromic Powder-Based Temperature-Adaptive Radiative Cooling Roofs. *Buildings* **2024**, *14*, 1745. https://doi.org/10.3390/buildings14061745

Academic Editor: Antonio Caggiano

Received: 10 May 2024
Revised: 5 June 2024
Accepted: 7 June 2024
Published: 10 June 2024

1. Introduction

Global warming not only endangers the balance of natural ecosystems but also threatens the survival of humans and animals. Reducing carbon emissions can effectively alleviate global warming, especially carbon emissions in the building sector, which account for 30–40% of total global carbon emissions [1–3]. As a passive cooling technique, radiative cooling can be achieved by exchanging heat with outer space through an atmospheric window (8–13 μm) without extra energy input, which effectively reduces building carbon emissions [4,5].

Radiative cooling materials are most convenient when employed as cool roofs in buildings, and they can reduce building energy consumption by 30–40% under different climates in China [6–8]. Many efforts have been made to prepare radiative cooling materials and to enhance the cooling energy efficiency for their application as cool roofs in buildings. Lin et al. [9] prepared a radiative cooling coating composed of a titanium dioxide–polydimethylsiloxane (TiO_2-PDMS) layer at the bottom and an aluminum oxide–polydimethylsiloxane (Al_2O_3-PDMS) layer at the top. Their study showed that the reflectivity in the solar spectrum and the emissivity in the atmospheric window of the coating are 92.2% and 95.3%, respectively. Furthermore, approximately 9.8 GJ per year of cooling energy is reduced by applying the proposed coating as the cool roof of a single-story office building in Mumbai. A sturdy aerogel with nano/microporous structures using cross-linked silica-hybridized cellulose acetate was proposed by Liu et al. [10] for achieving radiative cooling. Their investigation indicated that the solar reflectivity and emissivity

in the atmospheric window of the proposed aerogel are 96% and 97%, respectively, which can produce an energy reduction of 13.87 kW/m^2 when applying the aerogel to a modeled baseline building in China. Chen et al. [11] investigated the energy savings potential of porous polymer radiative cooling coatings as rooftops for concrete-based roofs, galvanized steel-based roofs, and commercial multilayered roofs in Hong Kong. The results showed that the annual cooling electricity savings of applying the porous polymer radiative cooling coating-based cool roofs are 3.23–47.71 kWh/m^2 compared to those of typical white coating-based roofs. Yang et al. [12] prepared a phosphate-activated geopolymer-based coating with a solar reflectivity of 0.9471 and a mid-infrared emissivity of 0.9634. Their experiments demonstrated that the surface temperature decreases by 3.8 °C below the ambient temperature under direct sunlight in Hong Kong. Compared to those of the budlings with a commercial cool roof and an ordinary cement roof, the energy consumption of the building with the proposed coating-based cool roof decreased by 266.61–627.75 kWh and 1240.87–2742.51 kWh, respectively. A cellulose nanocrystal aerogel grating (CAG) prepared by Cai et al. [13] achieved a solar reflectivity of 97.4% and an atmospheric window emissivity of 94%. Their study showed that 10.5 °C of sub-ambient cooling is achieved under a solar irradiance of 620 W/m^2. Furthermore, their simulation using EnergyPlus also indicated that 47% of the global cooling energy consumption occurs every year. A radiative cooling coating with a reflectivity of 97.4% and an emissivity of 94.4% was proposed by Yang et al. [14] based on calcined zeolite and polyurea. Their results indicated that the surface temperature of the proposed coating can be reduced by 4.4 °C under direct sunlight in summer. Furthermore, an average efficiency of 13.3% can be achieved for the application of a coating-based cool roof in a five-story building in China. A metamaterial-based radiative cooling film with a mid-infrared emissivity of 0.91 and a solar reflectivity of 0.92 was adopted by Wang et al. [15] as a cool roof of warehouses in Greenville, Cairo, Jimma, and Mexico. Their study showed that the annual energy consumption of a warehouse can be reduced by 22.4% in Greenville, 21.2% in Cairo, 53.0% in Jimma, and 65.2% in Mexico.

Although radiative cooling-based cool roofs can effectively reduce building energy consumption, radiative cooling remains in a cooling mode throughout the year and increases the heating load during the heating season. This also means that some of the cooling benefits will be offset by the heating penalty during the heating season.

Recently proposed temperature-adaptive radiative cooling (TARC) materials can adaptively change the solar reflectivity and/or the atmospheric window emissivity, accounting for changes in the ambient temperature and providing a possible solution to the increased heating load in the heating season caused by continuous daytime radiative cooling [16]. A similar method of applying phase change thermal storage material-based windows in buildings by Michał et al. [17] has demonstrated a 29.4% reduction in heating energy through windows in summer compared to that of ordinary windows. To alleviate the increased heating load caused by daytime radiative cooling, a passive cooling/heating double-effect material was proposed by our group in 2020 [18] based on polymers embedded with vanadium dioxide (VO_2) and dielectric particles. Then, two VO_2-based TARC materials were reported on 17 December 2021: (1) Tang et al. [19] developed a VO_2-based TARC coating in which the reflectivity and emissivity vary adaptively with changes in the ambient temperature. Their investigation indicated that the emissivity of the proposed TARC coating can change from 0.20 to 0.90, accounting for a phase transition temperature of 22 °C. The annual energy consumption of a typical residential building with TARC coating-based roofs in Maryland, U.S., can be reduced by 22.4 MJ/m^2 compared to that of a building with asphalt shingle (AS) roofs. (2) A thermochromic glass with passive radiative cooling regulation based on VO_2 was proposed by Wang et al. [20]. They experimentally demonstrated that the emissivity changes from 0.21 to 0.61 at a phase transition temperature of 60 °C. Furthermore, their simulation indicated that a maximum annual energy savings of 324.6 MJ/m^2 can be achieved by replacing low-E glass with the proposed thermochromic glass for a twelve-floor office building in seven different climates in the U.S. Since then, many researchers have devoted themselves to the study of TRAC.

Zhang et al. [21] fabricated a VO_2-based smart window whose mid-infrared emissivity could be adaptively switched from 0.35–0.68, accounting for a phase transition temperature of 20 °C. The experimental results showed that the indoor temperature of buildings with smart windows can decrease by 3.8 °C under a solar irradiance of 500 W/m^2 compared to that of buildings with regular glass windows. A scalable self-adaptive radiative cooling film was fabricated by Huang et al. [22] by incorporating core–shell nanoparticles of VO_2 into a polyethylene (PE) matrix. The results showed that 0.09 $kgCO_2/m^2$ of carbon emissions can be achieved by applying the proposed film on the roof of an eighteen-story residential building in Jan. Jinan, China. Wang et al. [23] proposed a thermochromic glass with multilayer anti-reflective coating/vanadium dioxide/anti-reflective coating (AIN/VO_2/AIN). Their results indicated that the proposed multilayer thermochromic glass works for heating and cooling when the temperature is below 20 °C or above 40 °C, respectively. This also means that the proposed multilayer thermochromic glass will change from heating to cooling when the temperature is increased from 20 °C (or lower) to 40 °C (or higher). Furthermore, a maximum energy savings of 12.13% can be achieved by applying the proposed multilayer thermochromic glass-based windows in an office building in Nanjing, China.

In addition to VO_2-based TARC materials, several TARC materials have also been proposed in existing studies, including hydrogel-based TARC materials [24,25], perovskite-based TARC materials [26,27], and other solution-based TARC materials [28]. However, most of these studies have focused on the preparation of TARC materials and their ability to change the temperature adaptively, with little attention given to the energy savings potential of these materials for their application in buildings. Although the energy-saving potential of VO_2-based TARC materials has been investigated, all VO_2-based TARC materials require doping with W and annealing. This not only increases the difficulty of fabricating VO_2-based TARC materials but also makes the performance of the annealed VO_2 extremely unstable [29]. To promote the application of TARC materials for improving building energy conservation, more attention should be given to the following two concerns: (1) the development of a simple-preparation TARC for large scalable application in buildings; and (2) a detailed analysis of energy performance for applying TARC in buildings.

To develop a TARC material with simple preparation, cost effectiveness, and large-scale application that can be widely used for improving building energy efficiency, this paper proposes a TARC coating based on a thermochromic powder. The process of preparing the proposed TARC coating was briefly introduced, and the performance parameters of the TARC coating (e.g., solar reflectivity and mid-infrared emissivity) were measured. Then, the heat transfer on the surface of the TARC coating was analyzed. Based on the measured performance parameters of the TARC coating, a typical two-story residential building with a roof area of 258.43 m^2 was modeled using EnergyPlus. Finally, the energy performance of applying the proposed TARC coating in buildings under different climates in China was discussed in detail. The flowchart of this study is shown in Figure 1.

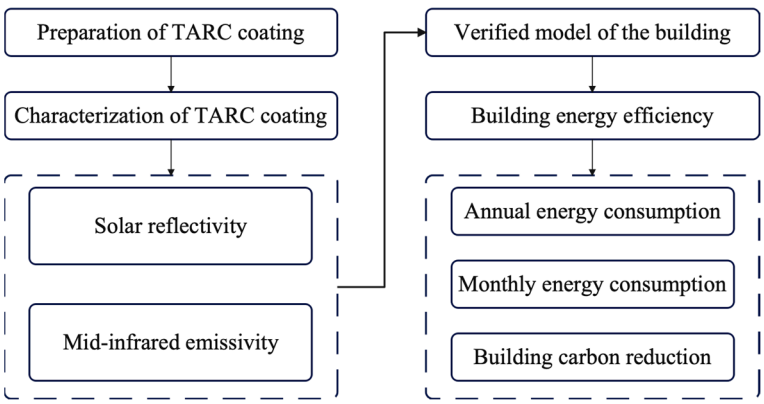

Figure 1. Flowchart of this study.

2. Methodology

2.1. Preparation of the TARC Coating

We prepared a TARC coating with a multilayer structure by doping a thermochromic powder (Shenzhen Tianjinli New Materials Technology Co., Ltd., Shenzhen, China) in ploymethylpentene (TPX) (Dongguan Huijie New Materials Co., Ltd., Dongguan, China) embedded with silicon dioxide (SO_2) (Dongguan Xinweijin Industrial Co., Ltd., Dongguan, China). The density, transmittance, and refractive index of the TPX are 0.84 g/cm^3, 0.93, and 1.46, respectively. SiO_2 is a colorless transparent crystal, whose reflectivity is 2–10% in the visible band. The specific process of preparation included the following steps: (1) SiO_2 particles with a diameter of 8 μm were dried in a vacuum oven for 8 h; (2) TPX was mixed with cyclohexane (Nanjing Wanqing Chemical Glass Instrument Co., Ltd., Nanjing, China) at a mass ratio of 0.08, and the mixture was stirred at 60 °C for 2.5 h until the TPX was completely dissolved (TPX dissolved solution). The cyclohexane is a colorless, pungent-smelling liquid, which dissolves polymers very well. (3) The TPX dissolved solution was allowed to stand until the temperature decreased to room temperature and was then mixed with the dried SO_2 particles at a volumetric ratio of 0.07 (TPX mixture dissolved solution). The TPX mixture dissolved solution was put into two beakers after 5 min and treated with a cell crusher. (4) The emission layer consisting of the TPX mixture dissolved solution was coated onto reflective layer of the aluminum foil using a coating machine (MSK-AFA-IIID-G, Shenyang Kejing Auto-instrument Co., Ltd., Shenyang, China). (5) The thermochromic power was added into the TPX mixture dissolved solution in another beaker and stirred continuously until the thermochromic powder was fully incorporated. Then, the solution was allowed to stand until all surface bubbles disappeared (thermochromic mixed solution). (6) The prepared thermochromic mixed solution was coated onto the emission layer, leading to a TARC coating with a multilayer structure. A schematic of the prepared TARC coating is shown in Figure 2.

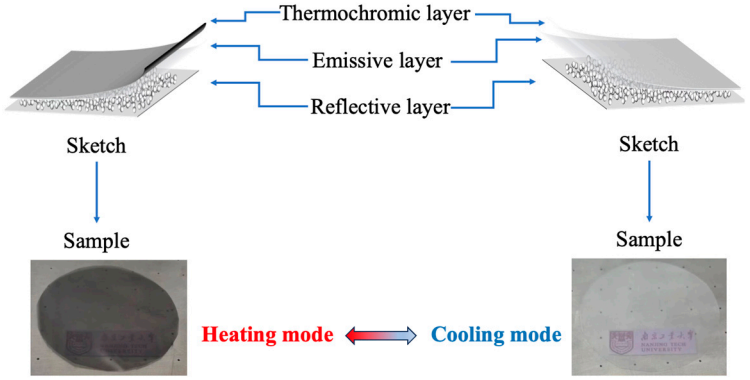

Figure 2. TARC coating.

As shown in Figure 2, the TARC coating appears transparent when the surface temperature is higher than the phase transition temperature. The TARC coating has high reflectivity in the solar spectrum and mid-infrared emissivity in this state. This also means that the TARC coating works in a cooling mode, reflecting solar irradiance while also exchanging heat with outer space through the transparent window to obtain cooling energy, thereby achieving sub-ambient radiative cooling. However, the TARC coating works in heating mode once the surface temperature is lower than the phase change temperature (25 °C), and it changes to a semitransparent coating with high solar absorptivity. This increases the absorption of solar irradiance and achieves heat collection.

2.2. Characterization of the TARC Coating

To determine the cooling and heating performance of the TARC coating, the solar reflectivity and mid-infrared emissivity were measured at the National Institute of Measurement and Testing Technology and Bohai University, respectively. The changes in the

reflectivity and emissivity of the TARC coating are shown in Figure 3. As shown in Figure 3, the average solar reflectivity in the solar spectrum (0.25–2.5 μm) is 0.73 in cooling mode. However, the average solar reflectivity decreases to 0.65 when the TARC coating changes to the heating mode. Especially for visible light wavelengths (0.38–0.78 μm), the average solar reflectivity decreases from 0.71 to 0.37 when the TARC coating changes from cooling mode to heating mode. This means that the absorption of solar irradiance at the visible light wavelength, which accounts for approximately 50% of the total solar irradiance, is significantly suppressed. Furthermore, the average emissivity of 0.93 in the atmospheric window is almost unchanged.

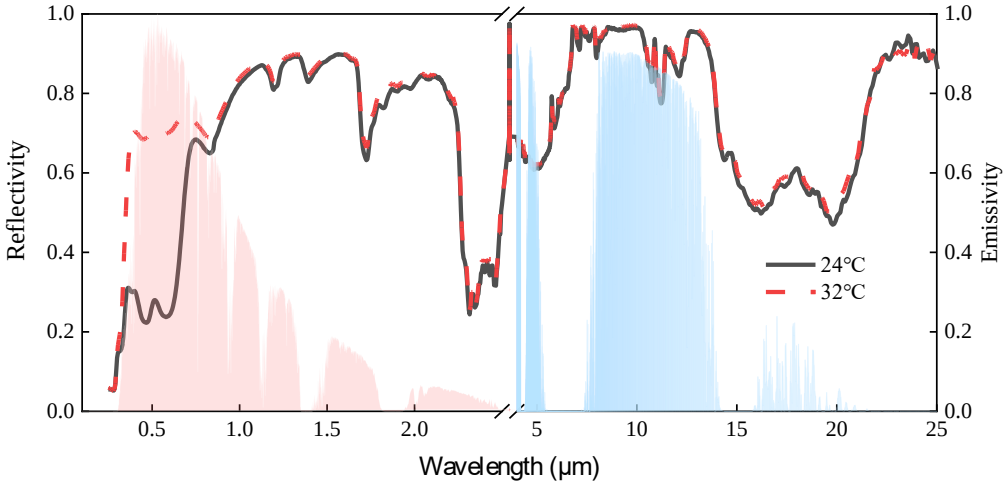

Figure 3. Reflectivity and emissivity of the TARC coating.

2.3. Modeling of the Building

To derive the energy efficiency potential for the application of the proposed TARC coating in buildings, a typical two-story residential building originating from the U.S. Department of Energy (DOE) building energy codes program [30] is adopted in this study. As shown in Figure 4, the modeled building with a roof area of 258.43 m^2 has dimensions of 12.13 m (length) × 9.10 m (width) × 5.79 m (height). A TARC coating/passive daytime radiative cooling (PDRC) coating is directly laid on the original roof (AS roof) to serve as the TARC roof/PDRC roof, and a split air conditioner is configured to supply supplemental cooling/heating to the building during the cooling/heating season. For the application of the TARC roof, the cooling and heating modes change adaptively with the roof surface temperature. Furthermore, other parameters of the modeled typical residential building can be found in Table 1.

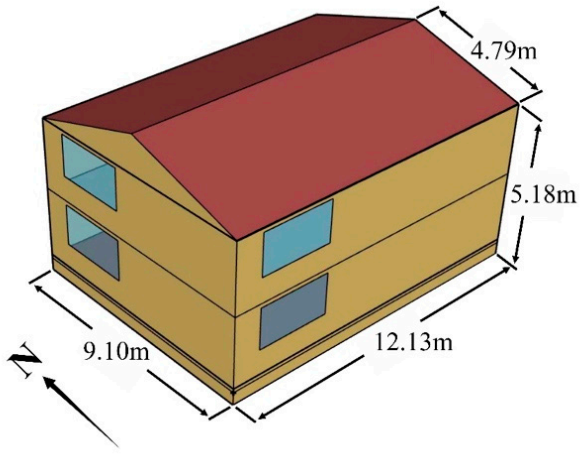

Figure 4. Sketch of the modeled building.

Table 1. Detailed parameters of the modeled building.

Item		Details
Window–wall ratio		12.78%
Occupants		3
Fresh air volume		30 m^3/h per person
Lighting density		8.5 W/m^2
Equipment power density		6.0 W/m^2
Interior design temperatures	Winter:	20 °C
	Summer:	27 °C
Roof	TARC	Cooling mode
		Reflectivity: 0.65
		Emissivity: 0.92
		Heating mode
		Reflectivity: 0.73
		Emissivity: 0.93
	PDRC [5]	Reflectivity: 0.92
		Emissivity: 0.91
	AS [6]	Reflectivity: 0.25
		Emissivity: 0.90

Since climate significantly impacts the energy performance of the TARC roof as well as changes in cooling and heating modes, five typical cities from all five climatic zones in China are adopted for this study, including Changchun, Beijing, Kunming, Chongqing, and Guangzhou. The criteria for the division of the different climatic zones are given in Ref. [31]. The TMY3 weather data provided by the DOE [32] are adopted in this investigation, and the envelopes of the modeled building are configured according to Ref. [33]. The detailed thermal performances of the envelopes can be found in Table 2.

Table 2. Required thermal performances of the envelopes for buildings in China [33].

City	Climatic Zone	Heat Transfer Coefficient (W/m^2·K)	
		Exterior Wall	Roof
Changchun	Severe cold zone	0.2	0.1
Beijing	Cold zone	0.25	0.2
Kunming	Moderate zone	0.4	0.25
Chongqing	Hot summer and cold winter zone	0.4	0.25
Guangzhou	Hot summer and warm winter zone	0.45	0.3

2.4. Heat transfer of the TARC Coating

The heat transfer of the TARC coating is shown in Figure 5, which includes the thermal radiation from the TARC coating (P_{rad}). the absorbed atmospheric radiation of the TARC coating (P_{atm}), the absorbed solar irradiance of the TARC coating (P_{sun}), the convection heat transfer between the TARC coating surface and the ambient air (P_{conv}), and the conduction heat transfer through the TARC coating (P_{cond}).

Then, the heat balance of the TARC coating can be expressed as follows:

$$P_{net} = P_{rad} - P_{atm} - P_{sun} - P_{conv} - P_{cond} \quad (1)$$

where P_{net} (W/m^2) is the net radiative power of the TARC coating.

Although the form of Equation (1) is the same as the heat balance of radiative cooling materials [34], there are differences in their physical meanings. This accounts for the change in the solar absorption under different operation modes. As shown in Figure 5, the solar

absorption increases significantly when the TARC coating switches from cooling mode to heating mode, thereby affecting the net radiative power.

The thermal radiation from the TARC coating (P_{rad}) can be derived from the following [5]:

$$P_{rad} = \int_0^{\frac{\pi}{2}} \pi \sin 2\theta d\theta \int_0^{\infty} I_B(T_{TARC}, \lambda) d\lambda \quad (2)$$

where θ (°) is the zenith angle; T_{TARC} (K) is the temperature of the TARC coating surface; λ (μm) is the wavelength; and I_B (T_{TARC}, λ) is the spectral radiance of a blackbody at temperature T_{TARC}, which is given as follows [6]:

$$I_B(T_{TARC}, \lambda) = 2hc^2 / \left(\lambda^5 (\exp(hc/\lambda k_B T_{TARC}) - 1)\right) \quad (3)$$

where h (J·s) is Planck's constant, 6.626×10^{-34}; c (m/s) is the speed of light, 299792458; and k_B (J/K) is Boltzmann's constant, $1.3806505 \times 10^{-23}$.

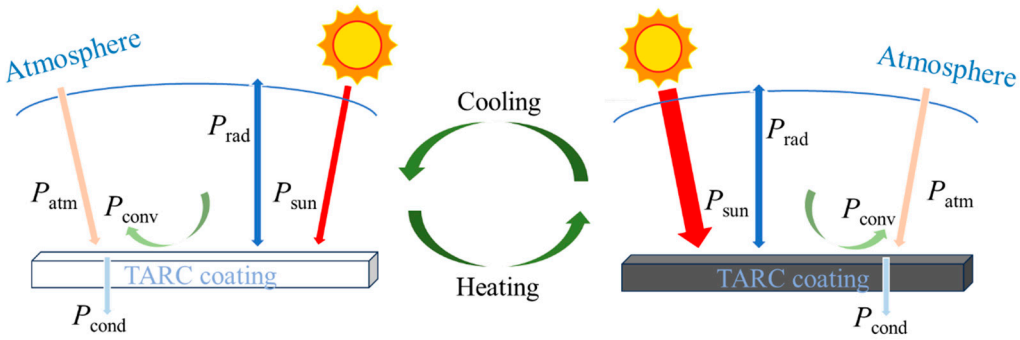

Figure 5. Heat transfer of the TARC coating.

The atmospheric radiation absorbed by the TARC coating (P_{atm}) can be calculated by the following equation [35]:

$$P_{atm} = \int_0^{\frac{\pi}{2}} \pi \sin 2\theta d\theta \int_0^{\infty} I_B(T_a, \lambda) \varepsilon_r(\lambda, \theta) \varepsilon_a(\lambda, \theta) d\lambda \quad (4)$$

where T_a (K) is the ambient temperature; $\varepsilon_r(\lambda, \theta)$ is the directional emissivity of the TARC coating; and $\varepsilon_a(\lambda, \theta)$ is the angle-dependent emissivity of the atmosphere.

The absorbed solar irradiance of the TARC coating (P_{sun}) can be derived from the following [36]:

$$P_{sun} = \int_0^{\frac{\pi}{2}} I_{AM1.5}(\lambda) \varepsilon(\lambda, \theta_{sun}) d\lambda \quad (5)$$

where $I_{AM1.5}$ is the solar irradiance relative to the normal solar spectrum; θ_{sun} (°) is the solar incidence angle; and $\varepsilon(\lambda, \theta_{sun})$ is the absorptivity at solar incidence angle θ_{sun} of the TARC coating.

The convective heat transfer between the TARC coating surface and the ambient air (P_{conv}) is determined by the following [37]:

$$P_{conv} = h_c (T_a - T_{TARC}) \quad (6)$$

where h_c (W/m^2·K) is the comprehensive heat transfer coefficient between the TARC coating and ambient air, which can be calculated according to Ref. [38].

The conduction heat transfer through the TARC coating (P_{cond}) is determined by the following [6]:

$$P_{cond} = \frac{\lambda_{roof} \Delta T}{\delta} \quad (7)$$

where λ_{roof} (W/m^2·K) is the thermal conductivity of the TARC coating and the original roof; ΔT (K) is the difference between the TARC coating and roof; and δ (m) is the thickness of the TARC coating and roof system.

2.5. Model Validation

To ensure the accuracy, the data in Ref. [19] are adopted to verify the model. Although the TARC coating used in Ref. [19] is a VO_2-based coating, the building in this study is the same as that in Ref. [19]. Therefore, the only work that needs to be carried out is to modify the properties (i.e., solar reflectivity and mid-infrared emissivity) of the TARC coating in this study to the same parameters as in Ref. [19]. This modification involves only the configuration of the emissivity and reflectivity of the TARC material. Thus, the accuracy of the model can be verified with the work in Ref. [19]. As shown in Figure 6, the relative error between the calculated annual cooling/heating energy consumption and the results in Ref. [19] is lower than 12%/17% for different cities in the U.S., which indicates that the established model can be used in the following study.

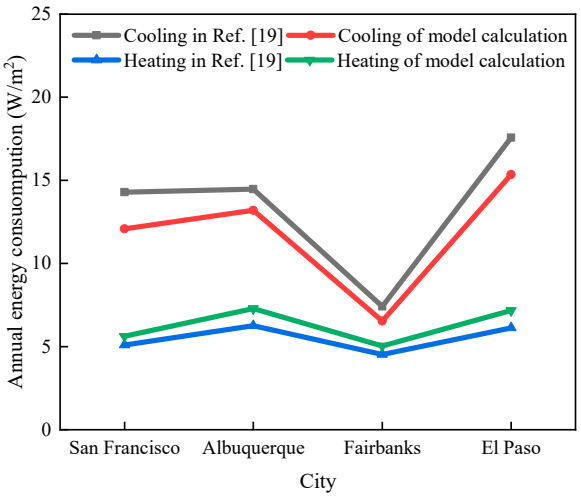

Figure 6. Comparison of annual energy consumption.

3. Results and Discussion

3.1. Effect of the TARC Roof on Annual Building Energy

To determine the energy-saving potential of applying TARC roofs to buildings, the energy consumption of buildings with TARC roofs is compared to that of buildings with AS roofs and PDRC roofs. A comparison of the energy consumption for buildings with the abovementioned roofs is shown in Figure 7.

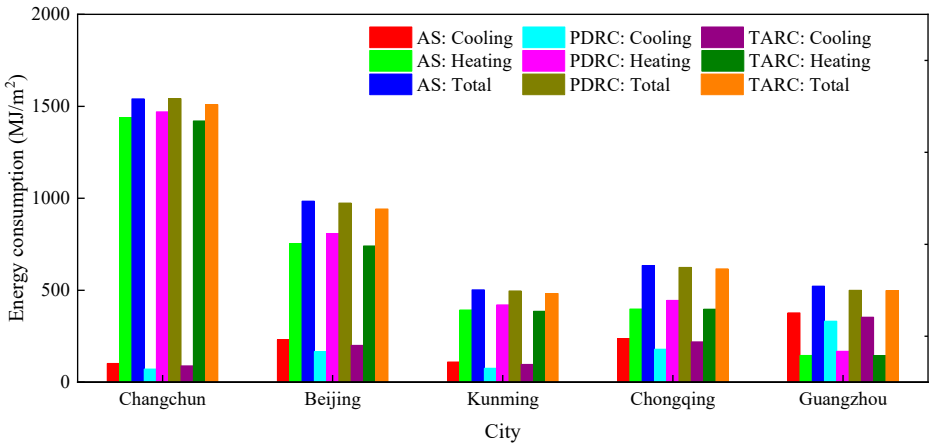

Figure 7. Energy consumption of buildings with different roofs.

As shown in Figure 7, the annual total energy consumption for buildings with TARC roofs decreased by 30.6 MJ/m^2 in Changchun, 43.0 MJ/m^2 in Beijing, 20.3 MJ/m^2 in Kunming, 17.8 MJ/m^2 in Chongqing, and 23.7 MJ/m^2 in Guangzhou compared to that for buildings with AS roofs. However, the annual total energy consumptions of buildings with TARC roofs are 31.8 MJ/m^2 lower than those with PDRC roofs in Changchun, 32.6 MJ/m^2 lower in Beijing, 14.4 MJ/m^2 lower in Kunming, 7.7 MJ/m^2 lower in Chongqing, and 2.0 MJ/m^2 lower in Guangzhou. This means that the TARC roof can further reduce building energy consumption compared to the AS roof or PDRC roof. In particular, energy savings are greatly improved when TARC roofs are used instead of PDRC roofs for cities with high heating demands in the winter (e.g., Changchun and Beijing). This is mainly because the continuous cooling of the PDRC roof all year leads to an increase in the heating load in winter. However, it should be noted that annual total building energy savings have deteriorated after the use of TARC roofs for cities with high cooling demands (e.g., Chongqing and Guangzhou), even though a minimum energy savings of approximately 7.7 MJ/m^2 and 2.2 MJ/m^2 can still be achieved in Chongqing and Guangzhou, respectively. This is mainly because the TARC coating is designed to achieve temperature adaptive changes, which requires considering the balance of cooling and heating power. This results in the solar reflectivity of the TARC coating in the cooling mode being lower than that of the PDRC coating, thereby reducing the net radiative cooling power. Thus, the energy savings potential decreases in cities with high cooling demands due to the decrease in reflectivity.

The annual space-conditioned electricity savings are also summarized in Table 3. Accounting for energy savings, the building electricity savings of applying TARC roofs in buildings are 8.6 kWh/m^2 in Changchun, 12.0 kWh/m^2 in Beijing, 5.7 kWh/m^2 in Kunming, 5.0 kWh/m^2 in Chongqing, and 6.6 kWh/m^2 in Guangzhou compared to those of the AS roof. Furthermore, the annual space-conditioned electricity consumption of buildings with TARC roofs can decrease by 8.9 kWh/m^2 in Changchun, 9.1 kWh/m^2 in Beijing, 4.0 kWh/m^2 in Kunming, 2.2 kWh/m^2 in Chongqing, and 0.6 kWh/m^2 in Guangzhou compared to that of buildings with PDRC roofs.

Table 3. Annual electricity savings for buildings with different roofs.

City	Compared to AS Roof (kWh/m^2)	Compared to PDRC Roof (kWh/m^2)
Changchun	8.6	8.9
Beijing	12.0	9.1
Kunming	5.7	4.0
Chongqing	5.0	2.2
Guangzhou	6.6	0.6

Accordingly, approximately 17.8–43.0 MJ/m^2 and 2.0–32.6 MJ/m^2 of energy consumption can be reduced for buildings with TARC roofs compared to those with AS roofs and PDRC roofs, respectively. Furthermore, TARC roofs are more suitable for buildings located in zones with high heating demands, while more building energy consumption can be achieved using PDRC roofs in buildings located in zones with high cooling demands.

3.2. Monthly Energy Consumption of Buildings with TARC Roofs

To determine the energy savings potential of applying TARC roofs in detail, the monthly energy consumption of buildings with different roofs is illustrated in Figure 8. As shown in Figure 8, the average monthly energy consumption of applying TARC roofs is generally lower than that of AS roofs. Compared to those of the buildings with AS roofs, the average monthly cooling energy reductions are 0.2–4.8 MJ/m^2 in Changchun, 0.4–7.5 MJ/m^2 in Beijing, 0.2–4.2 MJ/m^2 in Kunming, 0.0055.5 MJ/m^2 in Chongqing, and 0.03–4.5 MJ/m^2 in Guangzhou. However, the cooling benefits of applying TARC are generally lower than those of PDRC roofs. Especially for the Jun. to Aug. in Changchun,

May to Sept. in Beijing, Jun. to Aug. in Kunming, Jun. to Sept. in Chongqing, and Apr. to Nov. in Guangzhou, in which the average monthly cooling energy consumptions increase by 5.6–6.8 MJ/m^2, 4.2–9.2 MJ/m^2, 6.7–7.3 MJ/m^2, 6.5–10.2 MJ/m^2, and 1.2–5.4 MJ/m^2, respectively. This is mainly because the mid-infrared emissivity of TARC roofs in cooling mode is reduced to balance the cooling and heating capacity in these modes. Although the application of TARC roofs deteriorates the cooling benefits, heating penalties are more effectively mitigated than they are for PDRC roofs.

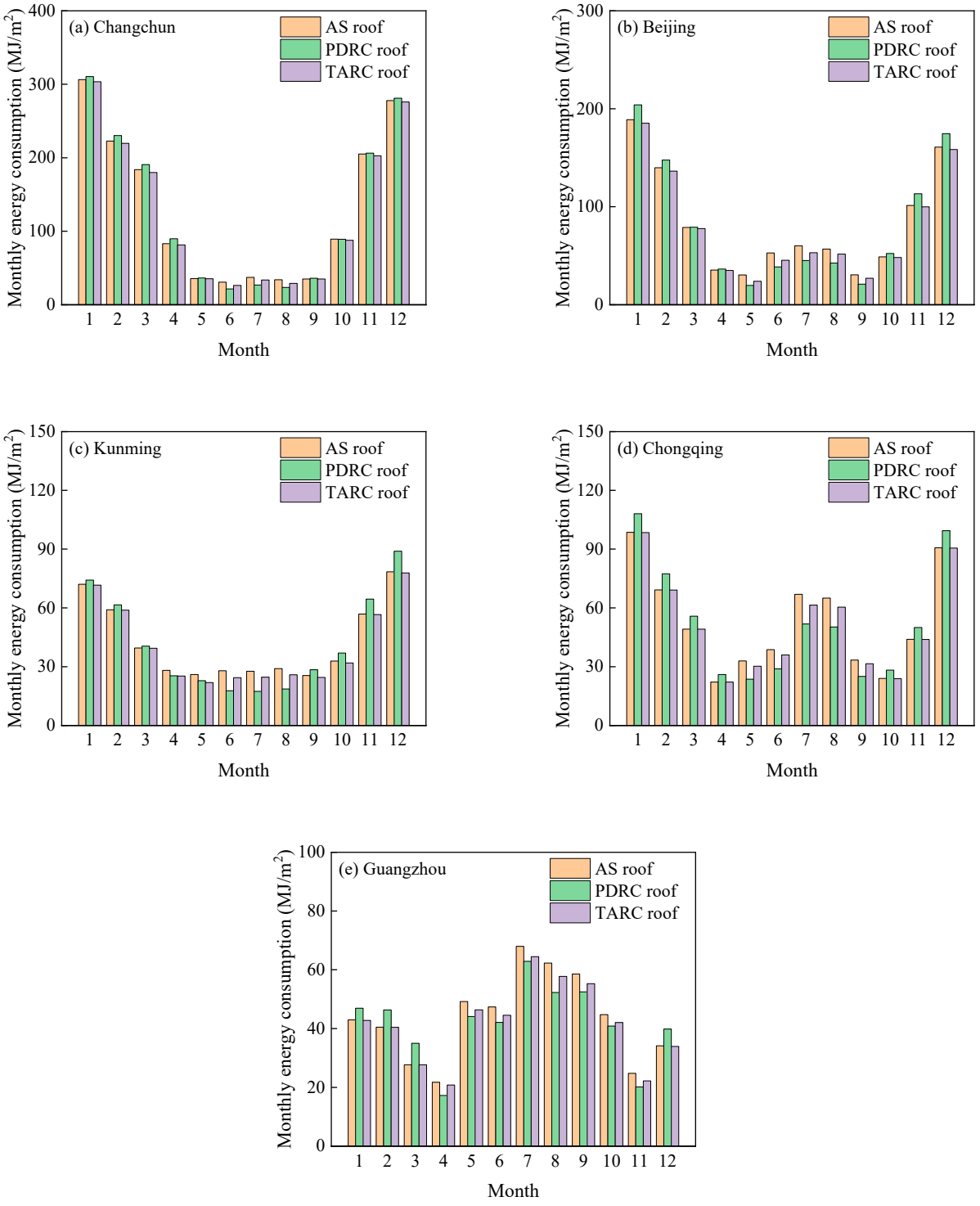

Figure 8. Monthly energy consumption for buildings with different roofs.

In addition, a comparison of the energy reduction for buildings with different roofs is also summarized in Table 4. As shown in Table 4, the energy savings of applying TARC roofs during the cooling season were 12.6/−17.3 MJ/m^2 in Changchun, 29.8/−34.1 MJ/m^2 in Beijing, 13.9/−20.1 MJ/m^2 in Kunming, 17.3/−40.0 MJ/m^2 in Chongqing, and 23.2/−21.3 MJ/m^2 in Guangzhou compared to those of AS roofs/PDRC roofs. However, the energy savings compared to those of AS roofs/PDRC roofs in the heating season are 18.0/49.1 MJ/m^2 in Changchun, 13.2/66.8 MJ/m^2 in Beijing, 6.5/34.5 MJ/m^2 in Kunming, 0.5/47.8 MJ/m^2 in Chongqing, and 0.5/23.3 MJ/m^2 in Guangzhou compared to those of AS roofs/PDRC roofs. It should be noted that heating energy consumption is almost unchanged for the application of TARC roofs in buildings located in Guangzhou and Chongqing compared to that for AS roofs. This is mainly because the two cities are in hot summer and warm winter and hot summer and cold winter climatic zones, respectively, which have low heating demand throughout the year.

Table 4. Comparison of energy reduction for buildings with different roofs.

City	Energy Reduction (MJ/m^2)			
	Compared to AS Roof		Compared to PDRC Roof	
	Cooling Season	Heating Season	Cooling Season	Heating Season
Changchun	12.6	18.0	−17.3	49.1
Beijing	29.8	13.2	−34.1	66.8
Kunming	13.9	6.5	−20.1	34.5
Chongqing	17.3	0.5	−40.0	47.8
Guangzhou	23.2	0.5	−21.3	23.3

3.3. Building Carbon Reduction of Applying TARC

The objective of reducing building energy consumption is to achieve carbon neutrality, and, thus, carbon emissions are also quantified in this study to further clarify the benefit of the application of TARC roofs in buildings. The reduction in carbon emissions can be derived from the following [39]:

$$E_{carbon} = \eta \times E_{ele} \quad (8)$$

where E_{carbon} (kgCO_2/m^2) is the space-conditioned carbon emissions; E_{ele} (kWh/m^2) is the space-conditioned energy; and η is the average emission coefficient accounting for the power grid of the city, which is presented in Table 5 [40].

Table 5. Average emission coefficients for energy consumption in the selected cities.

City	Emission Factors (kg CO_2/kWh)
Changchun	0.7769
Beijing	0.8843
Kunming	0.5271
Chongqing	0.5257
Guangzhou	0.5271

As shown in Figure 9, the annual carbon emissions reductions caused by applying the TARC roof are 23.8 kgCO_2/m^2 in Changchun, 38.0 kgCO_2/m^2 in Beijing, 10.7 kgCO_2/m^2 in Kunming, 9.4 kgCO_2/m^2 in Chongqing, and 12.5 kgCO_2/m^2 in Guangzhou compared to those caused by applying the AS roof. Furthermore, the annual carbon emissions of applying TARC roofs decreased by 24.7 kgCO_2/m^2 in Changchun, 28.9 kgCO_2/m^2 in Beijing, 7.6 kgCO_2/m^2 in Kunming, 4.1 kgCO_2/m^2 in Chongqing, and 1.0 kgCO_2/m^2 in Guangzhou in this model.

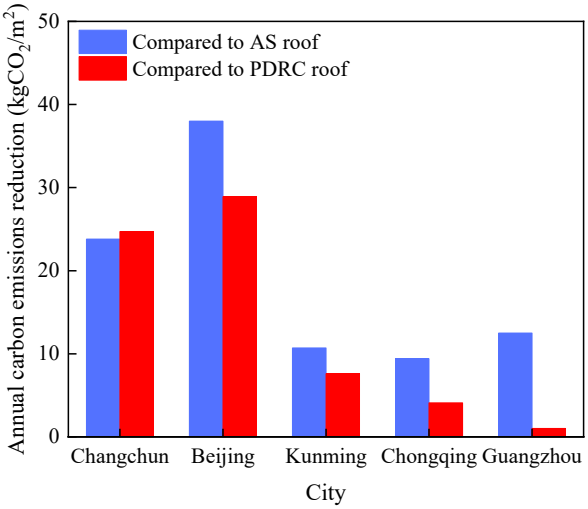

Figure 9. Carbon emissions reduction of applying the TARC roof.

To further indicate the differences in carbon emissions for buildings with different roofs, annual space-conditioned carbon emissions are also given in Table 6. As shown in Table 6, the carbon emissions of the buildings with TARC roofs are significantly lower than those with AS roofs and PDRC roofs. However, although the application of PDRC roofs can reduce carbon emissions from cooling, it also leads to an increase in carbon emissions from heating compared to that of the AS roof. Especially for Guangzhou, the annual carbon emissions of the AS roof and PDRC are identical, but the initial cost of applying the PDRC roof is greater than that of applying the AS roof, which limits its application in hot summer and cold winter zones. Compared with those of the AS roof, the carbon emissions from applying the TARC roof for both cooling and heating are lower, which demonstrates the significant carbon emissions reduction potential of the TARC roof. However, it should also be noted that although the annual carbon emissions of applying TARC roofs are lower than those of PDRC roofs, they are mainly due to the mitigation of heating penalties. However, the carbon emissions from cooling still increase.

Table 6. Annual space-conditioned carbon emissions.

City	Annual Carbon Emission ($kgCO_2/m^2$)								
	AS Roof			PDRC Roof			TARC Roof		
	Cooling	Heating	Total	Cooling	Heating	Total	Cooling	Heating	Total
Changchun	79.0	1117.8	1196.8	55.8	1141.9	1197.7	69.3	1103.8	1173.0
Beijing	204.0	666.7	870.7	147.5	714.0	861.6	177.7	655.0	832.7
Kunming	58.3	206.8	265.0	40.4	221.5	261.9	51.0	203.4	254.3
Chongqing	124.5	209.0	333.6	94.4	233.9	328.3	115.4	208.8	324.2
Guangzhou	198.5	76.5	275.1	175.0	88.6	263.6	262.6	76.3	262.6

4. Conclusions and Outlook

This paper proposes a thermochromic powder-based TARC coating, and a typical two-story residential building is modeled to determine the energy efficiency of the proposed TARC coating. Furthermore, the building energy efficiency enhancement of applying TARC roofs under different climates in China is discussed via comparisons with AS roofs and PDRC roofs. Compared to those for buildings with AS roofs and PDRC roofs in China, the main conclusions are as follows: (1) the energy consumptions for buildings with TARC roofs can be reduced by approximately 17.8–43.0 MJ/m^2 and 2.0–32.6 $MJ/m^{2,}$ respectively; (2) the annual carbon emissions reductions are 9.4–38.0 $kgCO_2/m^2$ and 1.0–28.9 $kgCO_2/m^2$, respectively.

This study demonstrates the energy efficiency of applying TRAC roofs in buildings. However, TARC roofs are more suitable for buildings located in zones with high heating demands, while more building energy consumption can be achieved using PDRC roofs in buildings located in zones with high cooling demands. Furthermore, the building envelope has a great impact on the energy consumption of TARC roof-based buildings. This paper only investigates the material's energy performance based on the code in China, and the building model should be modified according to the code for countries where the buildings are located.

Author Contributions: Conceptualization, K.Z.; methodology, K.Z.; software, G.S.; validation, G.S. and K.Z.; formal analysis, G.S.; investigation, G.S. and K.Z.; writing—original draft preparation, G.S.; writing—review and editing, K.Z., F.X., Z.Z., S.J. and Y.G.; supervision, K.Z.; project administration, K.Z.; funding acquisition, K.Z. All authors have read and agreed to the published version of the manuscript.

Funding: This research was funded by the National Natural Science Foundation of China, grant number 51878342.

Data Availability Statement: The data presented in this study are available on request from the corresponding author. The data are not publicly available due to privacy.

Conflicts of Interest: The authors declare no conflicts of interest.

Abbreviations

AS	Original roof	PDMS	Polydimethylsiloxane
PDRC	Passive daytime radiative cooling	PE	Polyethylene
TARC	Temperature-adaptive radiative cooling	TPX	Ploymethylpentene

References

1. Li, R.; You, K.R.; Cai, W.G.; Wang, J.B.; Liu, Y.; Yu, Y.H. Will the Southward Center of Gravity Migration of Population, Floor Area, and Building Energy Consumption Facilitate Building Carbon Emission Reduction in China. *Build. Environ.* **2023**, *242*, 110576. [CrossRef]
2. Kwok, K.Y.G.; Kim, J.; Chong, W.K.O.; Ariaratnam, S.T. Structuring a Comprehensive Carbon-Emission Framework for the Whole Lifecycle of Building, Operation, and Construction. *J. Archit. Eng.* **2016**, *22*, 04016006. [CrossRef]
3. Nutakki, T.U.K.; Kazim, K.W.U.; Alamara, K.; Salameh, T.; Abdelkareem, M.A. Experimental Investigation on Aging and Energy Savings Evaluation of High Solar Reflective Index (Sri) Paints: A Case Study on Residential Households in the GCC Region. *Buildings* **2023**, *13*, 419. [CrossRef]
4. Li, H.R.; Zhang, K.; Shi, Z.J.; Jiang, K.Y.; Wu, B.Y.; Ye, P.L. Cooling Benefit of Implementing Radiative Cooling on a City-Scale. *Renew. Energy* **2023**, *212*, 372–381. [CrossRef]
5. Jiang, K.Y.; Zhang, K.; Shi, Z.J.; Li, H.R.; Wu, B.Y.; Mahian, O.; Zhu, Y.T. Experimental and Numerical Study on the Potential of a New Radiative Cooling Paint Boosted by SiO_2 Microparticles for Energy Saving. *Energy* **2023**, *283*, 128473. [CrossRef]
6. Ma, M.Q.; Zhang, K.; Chen, L.F.; Tang, S.H. Analysis of the Impact of a Novel Cool Roof on Cooling Performance for a Low-Rise Prefabricated Building in China. *Build. Serv. Eng. Res. Technol.* **2020**, *42*, 26–44. [CrossRef]
7. Zhuang, Z.Y.; Yang, X.B.; Xie, K.; Tang, M.Y.; Xu, Y.B.; Ben, X.Y. The Mathematical Modeling and Performance of Sky Radiative Coolers. *Buildings* **2023**, *13*, 2972. [CrossRef]
8. Xiang, M.L.; Liao, Y.X.; Jia, Y.H.; Zhang, W.T.; Long, E.S. Summer Thermal Challenges in Emergency Tents: Insights into Thermal Characteristics of Tents with Air Conditioning. *Buildings* **2024**, *14*, 710. [CrossRef]
9. Lin, K.X.; Du, Y.W.; Chen, S.R.; Chao, L.K.; Lee, H.H.; Ho, C.T.; Zhu, Y.H.; Zeng, Y.J.; Pan, A.Q.; Yan, T.C. Nanoparticle-Polymer Hybrid Dual-Layer Coating with Broadband Solar Reflection for High-Performance Daytime Passive Radiative Cooling. *Energy Build.* **2022**, *276*, 112507. [CrossRef]
10. Liu, Y.M.; Bu, X.H.; Liu, R.Q.; Feng, M.X.; Zhang, Z.W.; He, M.; Huang, M.J.; Zhou, Y.M. Construction of Robust Silica-Hybridized Cellulose Aerogels Integrating Passive Radiative Cooling and Thermal Insulation for Year-Round Building Energy Saving. *Chem. Eng. J.* **2024**, *481*, 148780. [CrossRef]
11. Chen, J.H.; Lu, L.; Gong, Q.; Wang, B.X.; Jin, S.G.; Wang, M. Development of a New Spectral Selectivity-Based Passive Radiative Roof Cooling Model and Its Application in Hot and Humid Region. *J. Clean. Prod.* **2021**, *307*, 127170. [CrossRef]
12. Ning, Y.; Xuan, Q.D.; Fu, Y.; Ma, X.; Lei, D.Y.; Niu, J.L.; Dai, J.G. Phosphate Activated Geopolymer-Based Coating with High Temperature Resistance for Sub-Ambient Radiative Cooling. *Sustain. Cities Soc.* **2024**, *100*, 104992.

13. Cai, C.Y.; Chen, W.B.; Wei, Z.C.; Ding, C.X.; Sun, B.J.; Gerhard, C.; Fu, Y.; Zhang, K. Bioinspired "Aerogel Grating Metasurfaces Durable Daytime Radiat. Cool. Year-Round Energy Savings". *Nano Energy* **2023**, *114*, 108625. [CrossRef]
14. Yang, S.S.; Lei, S.; Wang, F.J.; Long, H.B.; Ou, J.F.; Amirfazli, A.; Baldelli, A. A Comprehensive Investigation of Zeolite/Polyurea Cooling Coating on Concrete for Building Energy Conservation. *Prog. Org. Coat.* **2024**, *188*, 108265. [CrossRef]
15. Wang, N.S.; Lv, Y.Y.; Zhao, D.L.; Zhao, W.B.; Xu, J.T.; Yang, R.G. Performance Evaluation of Radiative Cooling for Commercial-Scale Warehouse. *Mater. Today Energy* **2022**, *24*, 100927. [CrossRef]
16. Giulia, U.; Gianluca, R.; Kwok, W.S.; Jie, F.; Mattheos, S. On the Energy Modulation of Daytime Radiative Coolers: A Review on Infrared Emissivity Dynamic Switch Against Overcooling. *Sol. Energy* **2020**, *209*, 278–301.
17. Michał, M.; Lech, L. The Impact of a Mobile Shading System and a Phase-Change Heat Store on the Thermal Functioning of a Transparent Building Partition. *Materials* **2021**, *14*, 14102512.
18. Zhang, K.; Chen, L.F.; Song, G.; Niu, X.F.; Li, F. Passive Cooling/Heating Double-Effect Material. International Patent WO2021120706A1, 24 June 2021.
19. Tang, K.; Dong, K.C.; Li, J.C.; Gordon, M.P.; Reichertz, F.G.; Kim, H.; Rho, Y.; Wang, Q.J.; Lin, C.Y.; Grigoropoulos, C.P.; et al. Temperature-Adaptive Radiative Coating for All-Season Household Thermal Regulation. *Science* **2021**, *374*, 1504–1509. [CrossRef] [PubMed]
20. Wang, S.C.; Jiang, T.Y.; Meng, Y.; Yang, R.G.; Tan, G.; Long, Y. Scalable Thermochromic Smart Windows with Passive Radiative Cooling Regulation. *Science* **2021**, *374*, 1501–1504. [CrossRef] [PubMed]
21. Zhang, R.; Li, R.Z.; Xu, P.; Zhong, W.H.; Zhang, Y.; Luo, F.; Xiang, B. Thermochromic Smart Window Utilizing Passive Radiative Cooling for Self-Adaptive Thermoregulation. *Chem. Eng. J.* **2023**, *471*, 144527. [CrossRef]
22. Huang, J.C.; Zhang, X.-k.; Yu, X.Y.; Tang, G.H.; Wang, X.Y.; Du, M. Scalable Self-Adaptive Radiative Cooling Film through VO_2-Based Switchable Core–Shell Particles. *Renew. Energy* **2024**, *224*, 120208. [CrossRef]
23. Wang, J.Y.; Li, G.; Zhao, D.L. Multi-Objective Optimization of an Anti-Reflection AlN/VO_2/AlN Thermochromic Window for Building Energy Saving. *Energy* **2024**, *288*, 129798. [CrossRef]
24. Min, X.Z.; Wang, X.Y.; Li, J.L.; Xu, N.; Du, X.R.; Zeng, M.Y.; Li, W.; Zhu, B.; Zhu, J. A Smart Thermal-Gated Bilayer Membrane for Temperature-Adaptive Radiative Cooling and Solar Heating. *Sci. Bull.* **2023**, *18*, 2054–2062. [CrossRef] [PubMed]
25. Guo, N.; Liu, S.Q.; Chen, C.X.; Song, C.X.; Mo, S.H.; Yan, H.J.; Chen, M.J. Outdoor Adaptive Temperature Control Based on a Thermochromic Hydrogel by Regulating Solar Heating. *Sol. Energy* **2024**, *270*, 112405. [CrossRef]
26. Jiang, N.; Chen, S.M.; Wang, J.T.; He, C.Y.; Fang, K.; Yin, H.L.; Liu, Y.T.; Li, Y.; Yu, D. Smart Thermally Responsive Perovskite Materials: Thermo-Chromic Application and Density Function Theory Calculation. *Heliyon* **2023**, *9*, e12845. [CrossRef] [PubMed]
27. Du, Y.W.; Liu, S.; Zhou, Z.W.; Lee, H.H.; Ho, T.C.; Feng, S.-P.; Tso, C.Y. Study on the Halide Effect of MA4PbX6·2H_2O Hybrid Perovskites–from Thermochromic Properties to Practical Deployment for Smart Windows. *Mater. Today Phys.* **2022**, *23*, 100624. [CrossRef]
28. Yan, C.Q.; Li, A.K.; Wu, H.L.; Tong, Z.P.; Qu, J.H.; Sun, W.; Yang, Z.W. Scalable and All-Season Passive Thermal Modulation Enabled by Radiative Cooling, Selective Solar Absorption, and Thermal Retention. *Appl. Therm. Eng.* **2023**, *221*, 119707. [CrossRef]
29. Makarevich, A.M.; Sobol, A.G.; Sadykov, L.; Sharovarov, D.I.; Amelichev, V.A.; Tsymbarenko, D.M.; Boytsova, O.V.; Kaul, A.R. Delicate Tuning of Epitaxial VO_2 Films for Ultra-Sharp Electrical and Intense IR Optical Switching Properties. *J. Alloys Compd.* **2021**, *853*, 157214. [CrossRef]
30. Wong, R.Y.M.; Tso, C.Y.; Chao, C.Y.H.; Huang, B.; Wan, M.P. Ultra-Broadband Asymmetric Transmission Metallic Gratings for Subtropical Passive Daytime Radiative Cooling. *Sol. Energy Mater. Sol. Cells* **2018**, *186*, 330–339. [CrossRef]
31. Tang, S.H.; Akkurt, N.; Zhang, K.; Chen, L.F.; Ma, M.Q. Effect of Roof and Ceiling Configuration on Energy Performance of a Metamaterial-based Cool Roof for Low-rise Office Building in China. *Indoor Built Environ.* **2021**, *30*, 1739–1750. [CrossRef]
32. Weather Date. Available online: https://energyplus.net/weather-region (accessed on 10 April 2024).
33. *GB 55015-2021*; Code for Building Energy Efficiency and Renewable Energy Utilization. Ministry of Housing: Beijing, China, 2021.
34. Yang, Y.; Long, L.S.; Meng, S.; Denisuk, N.; Chen, G.Z.; Zhu, L.P. Bulk Material Based Selective Infrared Emitter for Sub-Ambient Daytime Radiative Cooling. *Sol. Energy Mater. Sol. Cells* **2020**, *211*, 110548. [CrossRef]
35. Huang, J.; Fan, D. Core-Shell Microspheres Hybridized Membrane for Light Emitting and Radiative Cooling. *J. Alloys Compd.* **2022**, *924*, 166480. [CrossRef]
36. Liu, J.W.; Zhang, D.B.; Jiao, S.F.; Zhou, Z.H.; Zhang, Z.F.; Gao, F. Preliminary Study of Radiative Cooling in Cooling Season of the Humid Coastal Area. *Sol. Energy Mater. Sol. Cells* **2020**, *208*, 110412. [CrossRef]
37. Kontoleon, K.J.; Eumorfopoulou, E.A. The Influence of Wall Orientation and Exterior Surface Solar Absorptivity on Time Lag and Decrement Factor in the Greek Region. *Renew. Energy* **2008**, *7*, 1652–1664. [CrossRef]
38. Wu, B.Y.; Zhang, K.; Ye, P.L.; Niu, Z.Y.; Song, G. Effect of Electronic and Phonon Properties on Polar Dielectric Embedded Polymer-Based Radiative Cooling Materials. *Sol. Energy Mater. Sol. Cells* **2018**, *224*, 371–381. [CrossRef]

39. Myint, N.N.; Shafique, M. Embodied Carbon Emissions of Buildings: Taking a Step Towards Net Zero Buildings. *Case Stud. Constr. Mater.* **2023**, *260*, 112473. [CrossRef]
40. Chen, Z.Y.; Dong, M.Y.; Wang, C.H. Passive Interfacial Photothermal Evaporation and Sky Radiative Cooling Assisted All-Day Freshwater Harvesting: System Design, Experiment Study, and Performance Evaluation. *Appl. Energy* **2023**, *475*, 146431. [CrossRef]